Biosensors and Bioelectronics 53 (2014) 117–122

Contents lists available at ScienceDirect

Biosensors and Bioelectronics

journal homepage: www.elsevier.com/locate/bios

Selective capture of human red blood cells based on blood group using long-range surface plasmon waveguides

Oleksiy Krupin [a], Chen Wang [b], Pierre Berini [c,d,*]

[a] Department of Biological and Chemical Engineering, University of Ottawa, 161 Louis Pasteur, Ottawa, Ontario, Canada K1N 6N5
[b] Department of Pathology and Laboratory Medicine, Mount Sinai Hospital, University of Toronto, 600 University Ave., Toronto, Canada M5G 1X5
[c] School of Electrical Engineering and Computer Science, University of Ottawa, 800 King Edward Ave., Ottawa, Canada K1N 6N5
[d] Department of Physics, University of Ottawa, 150 Louis Pasteur, Ottawa, Canada K1N 6N5

ARTICLE INFO

Article history:
Received 30 July 2013
Received in revised form
22 September 2013
Accepted 24 September 2013
Available online 29 September 2013

Keywords:
Optical biosensor
Long-range surface plasmon-polariton
Waveguide
Human red blood cells
CYTOP
Blood group detection

ABSTRACT

An optical biosensor based on long-range surface plasmon-polariton waveguides is applied to the detection of blood group antigen A on whole erythrocytes. The biosensor consists of straight gold waveguides embedded in CYTOP with an etched fluidic channel. The gold waveguides were functionalized with immunoglobulin G against blood group A (anti-A IgG) by forming a self-assembled monolayer (SAM) of 16-mercaptohexadecanoic acid (16-MHA) and then conjugating the anti-A IgG through carbodiimide chemistry. In order to demonstrate anti-A surface selectivity, solutions of O-type, B-type, A-type and AB-type red blood cells (RBCs) were sequentially injected over an anti-A functionalized waveguide. Surfaces were regenerated by lysing attached cells with distilled/deionized water (DDI H_2O). The efficiency of surface regeneration with DDI H_2O was very high as determined by performing six sequential binding/regeneration cycles of A RBC capture on the same anti-A surface. Also, five solutions of different A RBC concentrations, ranging from 1.14×10^5 cells/ml to 1.83×10^6 cells/ml, were injected over an anti-A surface to determine the limit of detection (LOD), which was found to be less than 3×10^5 cells/ml. Finally, the response produced by a single cell bound to a waveguide was determined by relating the number of bound cells to the response produced, from which the signal-to-noise ratio for single cell detection was determined to be ~95. The waveguides are promising as simple, low-cost and compact transducers, functionalized using standard thiol-based chemistries, for the selective detection of cells.

1. Introduction

Major appealing features of optical biosensors are their ability to perform analyte detection without labelling biomolecules and monitoring binding events in real-time (Cooper, 2002). Non-labelled detection (*e.g.* no fluorescent dyes) helps in reducing labour and provides a native environment for molecular interaction. Real-time detection allows for extracting binding kinetics from the data, which is of interest for drug discovery and the pharmaceutical sector. Only a monolayer of a ligand on the surface is required for capturing analyte, substantially reducing the demand for expensive biochemicals, such as antibodies.

Surface plasmon resonance (SPR) biosensors are currently the most common optical sensors on the market. SPR typically utilizes the Kretschmann–Raether configuration, which consists of a prism with a thin layer of gold deposited on one face. A transverse magnetic (TM) optical beam is incident onto the prism at an angle of incidence such that surface plasmons are excited on the gold film at its interface with the sensing solution (SPR angle), and as a result, the intensity of the reflected beam is lowest. The SPR angle is dependent on the local refractive index along the gold-solution interface. Upon analyte binding to the surface, the SPR angle changes producing changes in reflected power which can be tracked and real-time binding events followed (Homola et al., 1999; Lofas, 2004).

Long-range surface plasmon-polaritons (LRSPPs) are surface plasmon waves that can propagate over appreciable lengths along metal slabs or stripes bounded by similar dielectrics (insulator–metal–insulator configuration). The propagation length of LRSPPs is ~2000 μm compared to that of single-interface SPPs which is ~80 μm (Berini, 2009). The penetration depth of the LRSPP fields is ~1 μm, thus significantly larger than that of single-interface SPPs used in conventional SPR (~200 nm), which is advantageous if large objects such as cells must be sensed, or if a dextran matrix is used to increase the loading of small molecules along this dimension (Berini, 2009). LRSPPs have been shown to improve performance in modified SPR prism-based sensors, where higher sensitivity to refractive index changes and bacterial sensing have been demonstrated (Slavík and Homola, 2007; Vala et al., 2009). Furthermore, the detection of changes in induced cellular morphology has been investigated using

* Corresponding author at: School of Electrical Engineering and Computer Science, University of Ottawa, 800 King Edward Ave., Ottawa, Canada K1N 6N5. Tel.: +1 613 562 5800x6316; fax: +1 613 562 5175.
E-mail address: berini@eecs.uottawa.ca (P. Berini).

0956-5663/$ - see front matter © 2013 Elsevier B.V. All rights reserved.
http://dx.doi.org/10.1016/j.bios.2013.09.051

LRSPPs (modified prism-based SPR) and found to be more sensitive than conventional SPR (Chabot et al., 2012). For LRSPPs to propagate, the refractive index (RI) of the dielectrics along the top and bottom surfaces of the metal slab or stripe must be similar (Breukelaar et al., 2006). Thus, polymers of low RI (CYTOP and Teflon) are usually employed in LRSPP sensors as the bottom cladding, in order to match the RI of biologically compatible fluids which are aqueous and have $n \approx 1.33$ (Slavík and Homola, 2007; Vala et al., 2009; Joo et al., 2010; Dostálek et al., 2007; Guo et al., 2008). Due to the optical confinement of LRSPPs on metal stripes in the plane transverse to the direction of propagation, different integrated circuits such as Mach–Zehnder interferometers, Y-junctions, S-bends and couplers are possible (Charbonneau et al., 2006; Boltasseva et al., 2005). Although single-interface SPPs are more surface sensitive, the increased propagation length of LRSPPs more than compensates for a lower sensitivity in an integrated circuit (Berini, 2008). Furthermore, LRSPPs can be excited by butt-coupling a polarization-maintaining (PM) fibre to the waveguide, allowing for miniaturisation and lower costs. Dielectric waveguides have also been explored for biosensing using silicon nitride (Kinrot, 2004; Shew et al., 2008; Heidman and Lambeck, 1999) and silicon-on-insulator (Xu et al., 2008).

The sensor, discussed in this paper, consists of Au straight waveguides embedded in CYTOP with an etched fluidic channel to provide fluid access to the waveguide surface. The sensor differs from prism-based LRSPP sensors in that the latter does not provide lateral confinement of the mode and requires a prism-coupling scheme for excitation. Compared to dielectric waveguides, the sensor utilizes Au stripes, and the mode of operation is a surface plasmon. As an application for biosensing, the rationale for using Au is the availability of well-known and well-controlled surface chemistries for functionalization with receptors. Generally, Au has following advantages: (1) it is historically the most studied surface for functionalization; (2) SAMs using alkane-thiols are quickly formed (80–90% within the first few minutes) and gives a good organized packing, which improves as gold 111 crystallinity increases; (3) it is chemically inert and does not oxidize; (4) the SAM formed on a Au surface is relatively stable and can last for a long period of time (Love et al., 2005); and (5) A complete regeneration down to the Au surface is possible (Balasubramanian et al., 2006). Other advantages of using Au as the sensing surface include the ability to perform electrochemical desorption of SAMs for toposelective functionalization (Tencer et al., 2009, 2012), and the availability of thermo-optical modulation (Gagnon et al., 2006; Nikolajsen et al., 2004), which could be exploited to improve the detection limit. Alternatively, SAM formation on SiO_2 requires alkylsalines which are moisture sensitive and harder to process.

We have shown previously the ability of such (bio)sensing waveguides to detect changes in bulk refractive index, the adsorption of Bovine Serum Albumin on carboxyl- and polyethylene glycol-terminated surfaces, and the selective capture of human red blood cells (Krupin et al., 2013). Conventional SPR sensors have also been used to detect human RBCs based on blood group (Quinn et al., 1997, 2000), and to extract binding kinetics of cells interacting with the functionalized surface (Li et al., 2008). The purpose of this paper is to provide deeper insight into human RBC detection based on blood group A antigen using LRSPP straight waveguides. Au waveguides were functionalized with antibodies against A antigen using carbodiimide chemistry on a 16-MHA formed SAM. Both A and AB RBCs contain A antigen incorporated into the cell membrane while B and O RBCs do not, providing a basis for differentiation between the blood groups. We also perform an A RBC concentration response to determine our limit of detection (LOD), we investigate surface regeneration at the A antibody level, and we demonstrate the detection of a few cells captured by the waveguide. Surface regeneration is important in order to reuse the same sensing device, which results in a reduction of costs for blood grouping. Single cell detection is important in cancer detection, *e.g.*, for detecting rare circulating tumour cells (CTC), when at an early and aggressive stage of cancer, tumour cells leach into the blood stream (Hayes et al., 2006).

2. Materials and methods

2.1. Chemicals:

2-Isopropanol semiconductor grade (IPA), 16-mercaptohexadecanioc acid (HS(CH2)15COOH), *N*-(3-Dimethylaminopropyl)-*N*′-ethylcarbodiimide hydrochloride (EDC), *N*-Hydroxysuccinimide sodium salt (NHS), acetone HPLC grade ≥ 99.9% and glycerol (electrophoresis grade), Phosphate buffered saline (PBS) 0.01 M, pH 7.4 were obtained from Sigma-Aldrich. PBS solution was prepared by dissolving packaged salts in 1 L of distilled/deionized (DDI H_2O) water. Distilled water was deionized using Millipore filtering

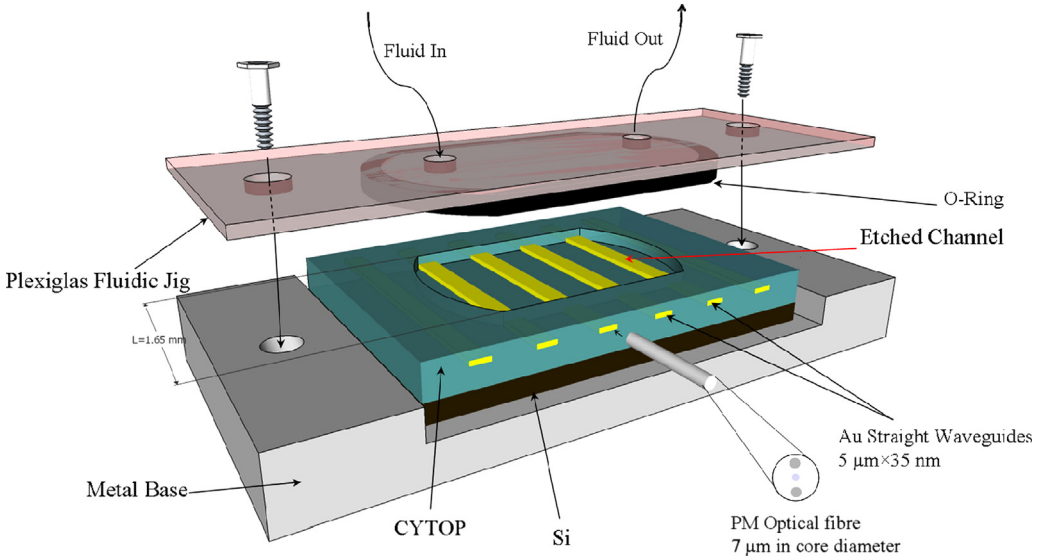

Fig. 1. Schematic representation of the sensor on the metal base with fluidic jig; the volume of the fluidic cell is 20 μL. (.).
Adapted from Krupin et al., 2013

membranes (Millipore, Milli-Q water system at 16 M Ω cm). Packed human red blood cells (groups A, B, O and AB) and antibodies against blood group A (Anti-A, Murine Monoclonal, Series 1, Immucor) were donated by Mount Sinai Hospital (Toronto).

2.2. Sensing device and fluidic integration

The sensing chip (3.8 mm × 6.4 mm) incorporates straight Au waveguides (5 μm wide and 35 nm thick) embedded in CYTOP. The etched fluidic channel is located in the middle of the chip, setting the sensing length to 1.65 mm as sketched in Fig. 1. For fluidic integration, the device is placed on a metal base and a Plexiglas jig with two holes and an O-ring (fluorocarbon, Apple Rubber Products Inc.), is attached by two Teflon screws to the metal base. Both the Plexiglas jig and the metal base are custom-made. This assembly provides a seal along with fluid access to the etched channel through Pico tubing (550 μm outer diameter, 250 μm inner diameter, IDEX) attached to the holes in the jig. The fluid was supplied by a syringe pump (PicoPlus, Harvard Apparatus).

The device was fabricated by spinning CYTOP on a 4″ Si wafer. Au features were lithographically defined thereon, and then another cladding of CYTOP was deposited. Fluidic channels were produced by etching down to the Au surface. The wafer was covered with photoresist and diced resulting in ~300 DIEs per wafer. Fabrication details can be found elsewhere (Asiri, 2012; Chiu et al., 2010). The optical interrogation setup and the general sensing approach are described in (Krupin et al., 2013). The flowrate for cell injection was investigated experimentally and selected as 20 μL/min. Slower flowrates resulted in cells settling and agglomerating in the fluidic tubing; whereas higher flowrates resulted in cells passing over the waveguide without binding (in the case of positive samples).The images of cells on a waveguide during experiment were taken by camera (FMA050, AmScope) installed on a microscope (SMZ645, Nikon).

2.3. Device preparation and functionalization

The dicing photoresist (SPR 220) was removed from the device by two sequential acetone baths (5 min and 30 min) followed by a thorough DDI H_2O and IPA wash. After N_2 drying, the device was cleaned again using an ultrasonic bath (FS20H, Fisher Scientific) in acetone for 30 s and then in IPA for 30 s to remove any possible debris that could have been formed during dicing. The device was dried with N_2 and placed in a UV/Ozone chamber (PSD-UV, Novascan) to remove any possible organic monolayer from the Au surface.

Prior to device integration with fluidics, the Au waveguides were functionalized with anti-A antibodies. A cleaned device was placed in a 2 mM IPA solution of 16-MHA for 2–24 h to allow a packed carboxyl-terminated SAM to form. After IPA washing and N_2 drying, the device was incubated in a DDI H_2O solution of 0.1 M EDC/NHS (1:1) for 15 min to activate the carboxyl group (Hermanson, 2008). In the final step, the device was cleaned with DDI H_2O, placed immediately into anti-A IgG (used as provided) for ~2 h to covalently attach IgGs to the surface, then washed with PBS and incorporated into the fluidic setup.

2.4. Analyte preparation

Previously we showed that the highest sensitivity to changes in RI at the waveguide surface occurs with a sensing solution of $n=1.3305$ (Krupin et al., 2013). Standard PBS buffer was doped with glycerol (7.235% w/w) and the RI of the buffer was measured with a prism-coupler based instrument at $\lambda_0=1312$ nm (Model 2010, Metricon, Prism 200-P1) to be $n=1.3305$. Packed RBCs were diluted with working buffer (PBS/Gly) and stored at 4 °C. Prior to an experiment, the cells were washed at 400 g in PBS/Gly using a micro-centrifuge (Micromax, Thermo Electric Corp.) 3 times for 2 min. The number of cells was counted using a haemocytometer (1483, Hausser Scientific) and the concentration of RBCs was worked out accordingly. All the solutions except for the ones containing cells were filtered through Millex-GP filters (PES membrane 0.22 μm).

3. Results and discussion

3.1. Anti-A surface selectivity

The sensing device and RBC solutions (4×10^7 cells/ml for all groups) were prepared as described above. All four blood groups (A, B, AB and O) were used independently as analyte and injected sequentially on the same anti-A functionalized waveguide. A typical response is shown in Fig. 2. The flow-rate was set to 65 μL/min during the entire experiment, except when the flow was stopped.

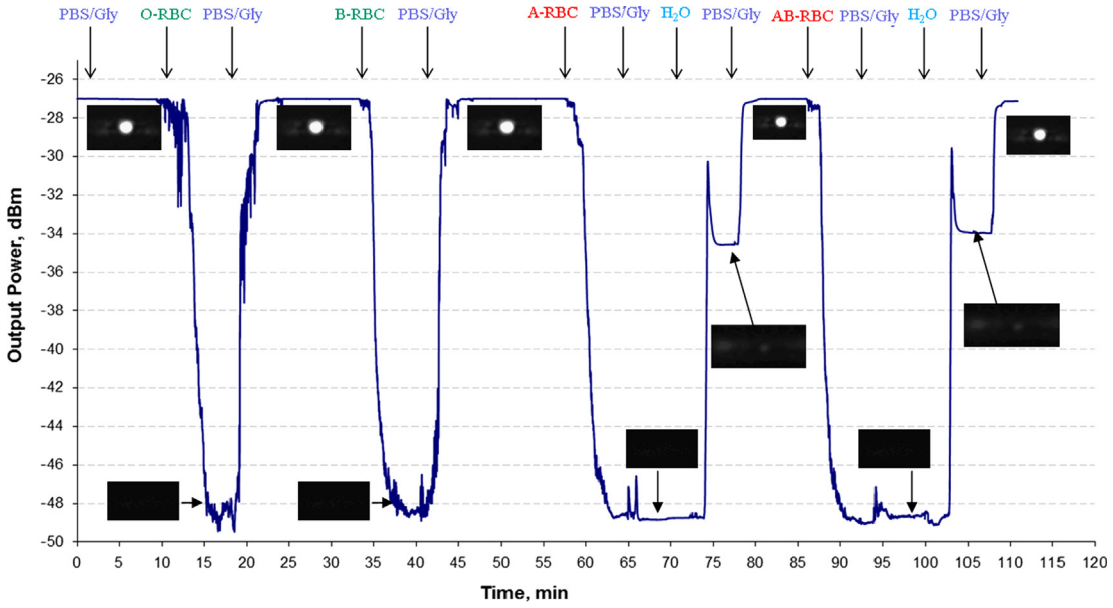

Fig. 2. Response of Au waveguides functionalized with anti-A IgG to RBCs belonging to the four blood groups (O, B, A and AB).

The baseline at −27 dBm output power level was established for 10 min, then O RBCs were injected and the flow was stopped to let the cells settle. Upon cell settling the mode disappeared completely and the power dropped to −49 dBm due to scattering and cut-off of the LRSPP induced by the cells on the waveguide. After 5 min the fluidic cell was flushed with PBS/Gly buffer to remove the erythrocytes and leading to recovery of the initial signal (25 min). The same procedure was performed with B RBCs: the cells were injected, the flow was stopped and after 5 min of signal loss, the buffer was re-injected to remove the cells (~35–45 min). Since the signal easily returned to the baseline level upon buffer injection, we conclude that both O and B RBCs did not specifically bind to the surface, and the signal loss was due to cells simply resting on the waveguide.

A RBCs were injected (55 min) and allowed to settle and react with the anti-A surface for 5 min. Afterwards, the fluidic cell was flushed with PBS/Gly buffer for ~8 min, but the power remained unchanged at −49 dBm throughout this time, indicating specific A RBC binding to the anti-A surface. The cells were lysed with DDI H_2O, and then the signal returned to the baseline level upon injection of PBS/Gly buffer (73–81 min). Lastly, the experiment was repeated with AB RBCs, also indicating specific cell binding (85–110 min). The noise spikes that are observed on O and B RBCs curves during injection/washing steps are due to cells passing across the waveguide and thus interrupting optical (LRSPP) power flow. The spikes that are present right after DDI H_2O injection are due to mixing of PBS/Gly solution and water.

3.2. Surface regeneration

An important property of any biosensor is its ability to be reused. In the present case, regeneration to the anti-A functionalized surface is of interest. DDI H_2O was used as a regeneration fluid, by lysing bound cells (due to low osmotic pressure), and possibly disrupting the antigen–antibody interaction, without damaging anti-A IgGs. We have performed several sequential binding/regeneration cycles in order to assess the potential of this simple regeneration approach—Fig. 3 summarises the results.

Before testing sensors, a large patch of Au (5 cm × 5 cm) deposited on CYTOP using the same fabrication method as for the sensors, was tested for regeneration. The patch was functionalized with anti-A in the same way as the sensors, and then the chip was placed in an A RBC solution (6×10^7 cells/ml) and allowed to incubate for ~15 min. The chip was removed from the A RBC solution and placed in clean PBS/Gly buffer (under gentle agitation) until only a monolayer of cells remained. Images were taken using a microscope (BH2-4MA, Olympus) at 50× magnification. Then the chip was washed with DDI H_2O to remove the attached cells (confirmed by microscope inspections) and returned to the container with A RBCs, thus completing one cycle. Nine such binding/regeneration cycles were performed sequentially on the same surface, with images being taken after the first and last A RBC binding, as shown in Fig. 3a and b. Both images show a high and indistinguishable density of cells per unit area suggesting successful DDI H_2O regeneration.

An anti-A functionalized sensor was tested using the same regeneration strategy applied to six binding/regeneration cycles. All cycles were performed sequentially under a 20 μL/min flow-rate and using a concentration of A RBCs of 4×10^6 cells/ml. A baseline was established over ~5 min, and then A RBCs were introduced. The first and last (6th) binding curves, shown in Fig. 3c and d, saturate at a similar power level of −39 and −38 dBm, respectively, indicating successful regenerations. To rule out non-specific binding, O RBCs (4×10^6 cells/ml) were injected after the last regeneration and

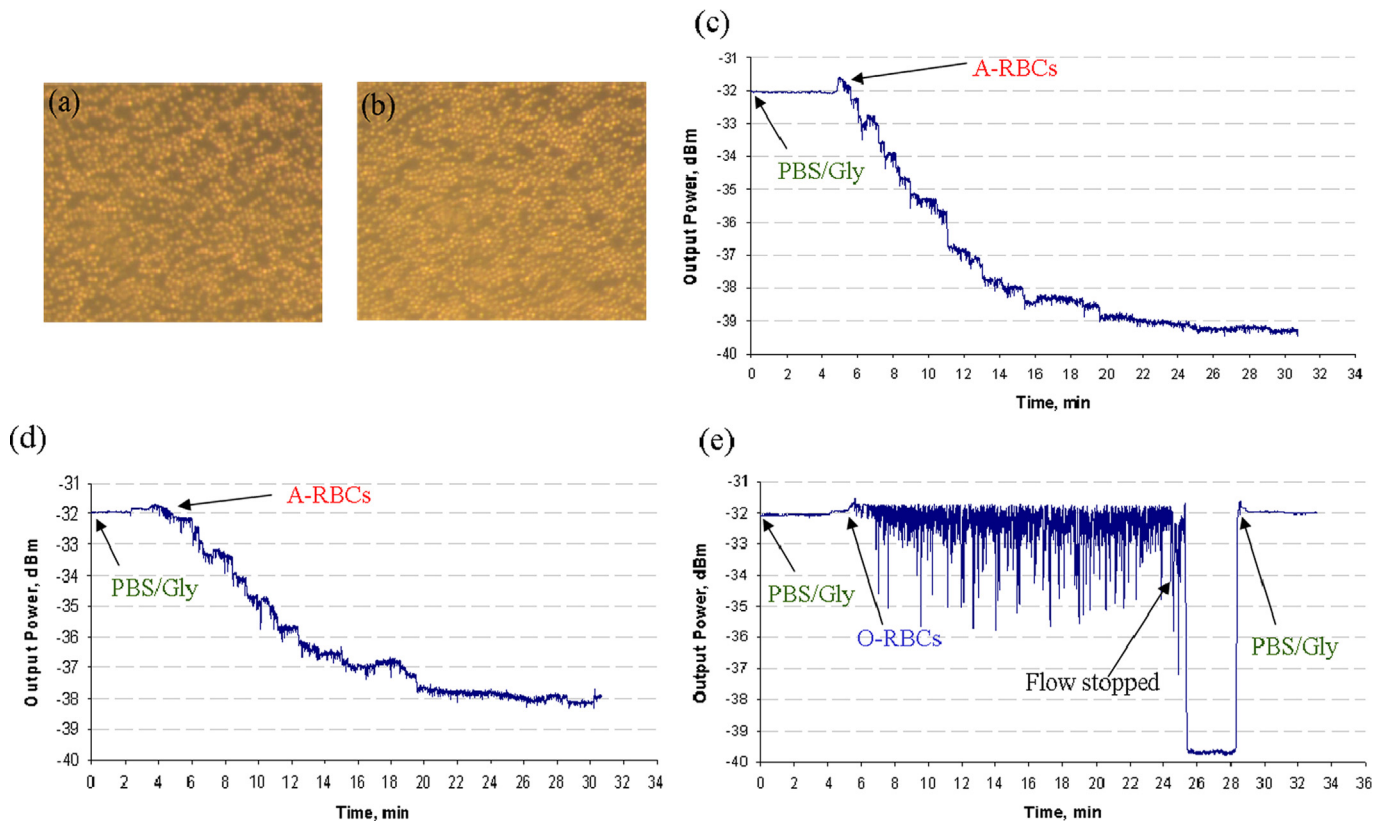

Fig. 3. Regeneration of anti-A IgG functionalized surfaces with DDI H_2O: (a) Large Au patch on CYTOP, 1st binding of A RBCs; (b) Large Au patch on CYTOP, 9th binding of A RBCs; (c) 1st binding curve of A RBCs to a sensor; (d) 6th binding curve of A RBCs to a sensor; and (e) final O RBC injection. All injection flow-rates were 20 μL/min. The concentration of cells used in Parts (a) and (b) was 6×10^7 cells/ml and that used in Parts (c) and (d) was 4×10^6 cells/ml.

allowed to settle for ~3 min. Subsequent injection of PBS/Gly buffer removed the cells from the waveguide, as indicated by recovery of the signal to the baseline level of −32 dBm in Fig. 3e.

3.3. Concentration limit of detection

In order to determine the concentration LOD for our biosensing scheme, solutions having different concentrations of A RBCs in buffer were injected on the same anti-A functionalized waveguide, using the DDI H_2O regeneration scheme of Section 3.2 between runs to regenerate the surface. The experiments were performed in a sequence of decreasing concentrations starting from 1.83×10^6 cells/ml with the last one being 1.14×10^5 cells/ml, which produced no response within a 20 min period; Fig. 4 summarises the results. Thus, the LOD can be estimated to be less than 3×10^5 cells/ml, which is several orders of magnitude lower than has been found for SPR (0.33×10^9 cells/ml) (Quinn et al., 1997). The observed noise spikes are due to cells drifting along the waveguide with a velocity higher than required for attachment. The step-like response is likely to be indicative of a single or few cells attaching to the surface. The most vivid example is the curve with 4.39×10^5 cells/ml concentration, where the downward step-like response is observed.

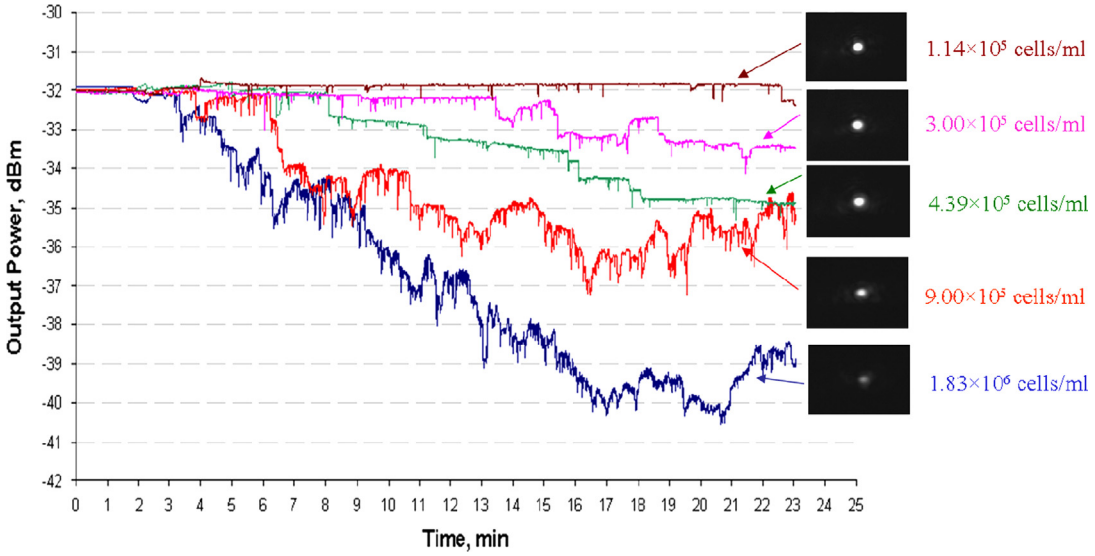

Fig. 4. Concentration responses of A RBC solutions on the same Au waveguide functionalized with anti-A IgG. All flow-rates were 20 μL/min.

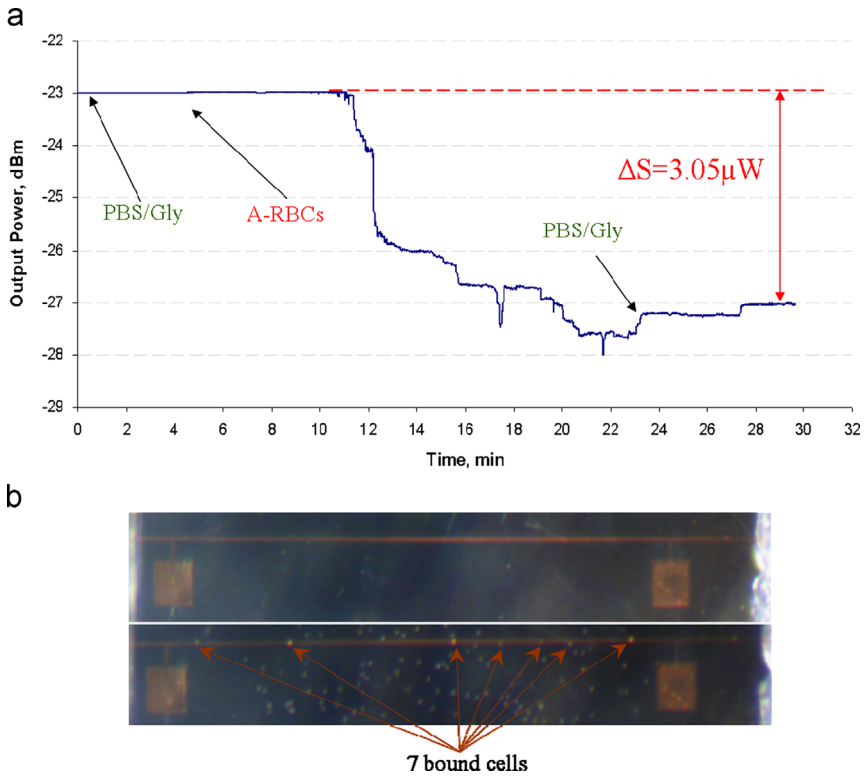

Fig. 5. Detection of single cells on a Au waveguide: (a) binding response of a A RBC solution (8×10^5 cells/ml) injected over an anti-A functionalized sensor; (b) images of the waveguide before (top) and after (bottom) the experiment.

3.4. Single cell detection

The step-like binding response under flow observed in the concentration response (Section 3.3) suggests that single cell detection is possible. An anti-A functionalized waveguide was exposed to an A RBC solution (8×10^5 cells/ml) under flow (20 μL/min) until a reasonable, but not complete, drop in signal was observed, as shown in Fig. 5a. At this point (~23 min) the fluidic cell was flushed with PBS/Gly buffer for 7 min at a flow-rate of 40 μL/min. Microscope images of the waveguide were taken before and after the experiment, as shown in Fig. 5b, and the number of bound cells after the experiment was counted. Seven bound cells produced a signal change of 3.05 μW, yielding a 0.43 μW power drop per cell. The baseline noise, taken as the standard deviation of the output power over time, was $\sigma = 4.5$ nW, so the signal-to-noise ratio for capturing a single cell on the waveguide is $S/N \sim 95$.

4. Conclusion

An optical biosensor based on straight Au waveguides operating with LRSPPs was applied to the selective detection of human red blood cells. Cells bearing A-antigen (A and AB RBCs) were successfully detected, whereas cells without this antigen (O and B RBCs) served as negative controls. The sensor thus demonstrated an ability to differentiate between blood groups containing A-antigen and blood groups lacking the antigen. Regeneration of the anti-A functionalized surface by injecting DDI H_2O to lyse bound cells was also demonstrated for several sequential binding cycles on the same surface with no significant changes being observed between the first and the last binding responses. The concentration LOD for A RBC detection was found to be less than 3×10^5 cells/ml. Finally, few-cell capture was demonstrated, and the signal-to-noise ratio for single-cell capture estimated as $S/N \sim 95$.

An advantage of this sensing technique over a standard clinical procedure based on an agglutination test is reduced antibody usage, which is practically insignificant in the sensor compared to an agglutination test. Miniaturization of the sensor is an advantage over conventional SPR sensors. Both of these features can lead potentially to cheap blood grouping procedures. The ability to sense a single captured cell can be of interest in other applications such as environmental sensing of bacteria, or for the detection of rare cells in medical applications.

Acknowledgments

The authors gratefully acknowledge NSERC (BiopSys Network) for funding, Ewa Lisicka-Skrzek, Michal Tencer, Asad Khan, Hamoudi Asiri, and Anthony Olivieri for assistance in carrying out the experiments.

References

Asiri, H., (Master's Thesis), Department of Chemistry and Biological Engineering, University of Ottawa, Ottawa,2012.
Balasubramanian, S., Revzin, A., Sirnonian, A., 2006. Electroanalysis 18, 1885–1892.
Berini, P., 2008. New Journal of Physics 10, 105010.
Berini, P., 2009. Advances in Optics and Photonics 1, 484–588.
Boltasseva, A., Nikolajsen, T., Leosson, K., Kjaer, K., Larsen, M.S., Bozhevolnyi, S.I., 2005. Journal of Lightwave Technology 23 (1), 413–422.
Breukelaar, I., Charbonneau, R., Berini, P., 2006. Journal of Applied Physics 100 (4), 43–104.
Chabot, V., Miron, Y., Grandbois, M., Charettea, P.G., 2012. Sensors and Actuators B: Chemical 174, 94–101.
Charbonneau, R., Scales, C., Breukelaar, I., Fafard, S., Lahoud, N., Mattiussi, G., Berini, P., 2006. Journal of Lightwave Technology 24 (1), 477–494.
Chiu, C., Lisicka-Skrzek, E., Tait, R.N., Berini, P., 2010. Journal of Vacuum Science and Technology B 28 (4), 729–735.
Cooper, M.A., 2002. Nature Reviews Drug Discovery 1, 515–527.
Dostálek, J., Kasry, A., Knoll, W., 2007. Plasmonics 2 (3), 97–106.
Gagnon, G., Lahoud, N., Mattiussi, G.A., Berini, P., 2006. Journal of Lightwave Technology 24 (11), 4391–4402.
Guo, J., Keathley, P.D., Hastings, J.T., 2008. Optics Letters 33 (5), 512–514.
Hayes, D.F., Cristofanilli, M., Budd, G.T., Ellis, M.J., Stopeck, A., Miller, M.C., Matera, J., Allard, W.J., Doyle, G.V., Terstappen, L.W.W.M., 2006. Clinical Cancer Research 12 (14), 4218–4224.
Heideman, R.G., Lambeck, P.V., 1999. Sensors and Actuators B: Chemical 61 (1–3), 100–127.
Hermanson, T.G., 2008. Bioconjugate Techniques, 2nd ed. Rockford, USA.
Homola, J., Yee, S.S., Gauglitz, G., 1999. Sensors and Actuators B: Chemical 54, 3–15.
Joo, Y.H., Song, S., Magnusson, R., 2010. Applied Physics Letters 97 (20), 201105.
Kinrot, N., 2004. Journal of Lightwave Technology 22 (10), 2296–2301.
Krupin, O., Asiri, H., Wang, C., Tait, R.N., Berini, P., 2013. Optics Express 21, 698–709.
Li, B., Chen, J., Long, M., 2008. Analytical Biochemistry 377, 195–201.
Lofas, S., 2004. Assay and Drug Development Technologies 2 (4), 407–415.
Love, J.C., Estroff, L.A., Kriebel, J.K., Nuzzo, R.G., Whitesides, G.M., 2005. Chemical Reviews 105 (4), 1103–1170.
Nikolajsen, T., Leosson, K., Bozhevolnyi, S.I., 2004. Applied Physics Letters 85 (24), 5833–5835.
Quinn, J.G., O'Kennedy, R., Smyth, M., Moulds, J., Frame, T., 1997. Journal of Immunological Methods 206, 87–96.
Quinn, J.G., O'Neill, S., Doyle, A., McAtamney, C., Diamond, D., MacCraith, B.D., O'Kennedy, R., 2000. Analytical Biochemistry 281, 135–143.
Shew, B.Y., Cheng, Y.C., Tsai, Y.H., 2008. Sensors and Actuators A: Physical 141 (2), 299–306.
Slavík, R., Homola, J., 2007. Sensors and Actuators B: Chemical 123, 10–12.
Tencer, M., Nie, H.Y., Berini, P., 2009. Journal of the Electrochemical Society 156 (12), J386–J392.
Tencer, M., Olivieri, A., Tezel, B., Nie, H.Y., Berini, P., 2012. Journal of the Electrochemical Society 159 (3), J77–J82.
Vala, M., Etheridge, S., Roach, J.A., Homola, J., 2009. Sensors and Actuators B: Chemical 139, 59–63.
Xu, D.X., Densmore, A., Delâge, A., Waldron, P., McKinnon, R., Janz, S., Lapointe, J., Lopinski, G., Mischki, T., Post, E., Cheben, P., Schmid, J.H., 2008. Optics Express 16 (19), 15137–15148.